Protein Crystallization Facilitated by Molecularly Imprinted Polymers

Emmanuel Saridakis[a], Sahir Khurshid[b], Lata Govada[b], Quan Phan[c], Daniel Hawkins[c], Gregg V. Crichlow[d], Elias J. Lolis[d], Subrayal M. Reddy[c,1] and Naomi E. Chayen[b,1]

[a] *Laboratory of Structural and Supramolecular Chemistry, Institute of Physical Chemistry, N.C.S.R. "Demokritos", Ag. Paraskevi, Athens 15310, Greece* [b] *Biomolecular Medicine, Department of Surgery and Cancer, Faculty of Medicine, Imperial College London, Sir Alexander Fleming Building, London SW7 2AZ, U.K* [c] *Chemical Sciences Division, Faculty of Health and Medical Science, University of Surrey, Guildford, Surrey GU2 7XH, U.K., and* [d] *Department of Pharmacology, Yale University, New Haven, CT 06520-806, USA..*

Corresponding Authors:

Professor Naomi E. Chayen
Biomolecular Medicine
Department of Surgery and Cancer
Faculty of Medicine
Imperial College London
Sir Alexander Fleming Building
London SW7 2AZ, UK

Tel: +44-207-594-3240
Fax: +44-207-594-3226
Email: n.chayen@imperial.ac.uk

and
Dr Subrayal M Reddy
Email: s.reddy@surrey.ac.uk

Emmanuel Saridakis[a], Sahir Khurshid[b], Lata Govada[b] contributed equally to this work.

To whom correspondence may be addressed. E-mail: s.reddy@surrey.ac.uk or n.chayen@imperial.ac.uk

Classification:

Major: Biological Sciences

Minor: Biophysics and Computational Biology

Abstract

We present a new initiative and its application, namely the design of molecularly imprinted polymers (MIPs) for producing protein crystals which are essential for determining high-resolution 3-D structures of proteins. MIPs, also referred to as 'smart materials' are made to contain cavities capable of rebinding protein, thus the fingerprint of the protein created on the polymer allows it to serve as an ideal template for crystal formation. We have shown that six different MIPs induced crystallization of nine proteins, yielding crystals in conditions that do not give crystals otherwise. The incorporation of MIPs in screening experiments gave rise to crystalline hits in 8-10% of the trials for three target proteins. These hits would have been missed using other known nucleants. MIPs also facilitated the formation of large single crystals at metastable conditions for seven proteins. Moreover, the presence of MIPs has led to faster formation of crystals in all cases where crystals would appear eventually and to major improvement in diffraction in some cases. The MIPs were effective for their cognate proteins and also for other proteins, with size-compatibility being a likely criterion for efficacy. Atomic Force Microscopy (AFM) measurements demonstrated specific affinity between the MIPs cavities and a protein-functionalised AFM tip, corroborating our hypothesis that due to the recognition of proteins by the cavities, MIPs can act as nucleation inducing substrates (nucleants) by harnessing the proteins themselves as templates.

\body

Molecularly imprinted polymers (MIPs) are polymers formed in the presence of a molecule that is extracted afterwards, thus leaving complementary cavities (or ghost-sites) behind. The molecular imprint remains as a memory effect in the gel after the molecule is removed, and the cavities exhibit highly selective rebinding of the given molecule (1, 2).

MIPs were initially used for separation and purification of small molecules such as enantio separation of racemic mixtures in chiral compounds (3), separation of carbohydrate derivatives (4) and in thin layer chromatography (5). More recently MIPs have become an important tool in the preparation of artificial recognition materials that are capable of mimicking natural systems (6, 7). In the context of proteins, MIPs have been used for protein purification/isolation applications (8), replacement of biological antibodies in immunoassays (9 and refs therein), catalysis (10) and biosensors for medicine (7 and refs therein). MIPs however, have never before been used to facilitate protein crystallization.

This study presents a new approach to the use of MIPs by harnessing them as surfaces for inducing the formation of protein crystals. Protein crystallization is vital to the success of structural biology as well as structural genomics/proteomics projects worldwide that have set out to determine the structures of more than 100,000 proteins. Obtaining useful crystals remains a major bottleneck to progress (11), thus it is crucial to design new and improved means of producing the desired crystals.

The ultimate way to obtain high quality crystals is to control their conception stage, namely their nucleation, which is the first step that determines the entire crystallization process (12). Once nucleated, crystal growth is optimal at metastable conditions, where crystals do not nucleate spontaneously but existing nuclei will grow in a controlled manner that will minimize structural defects. Crystallization at metastable conditions can be induced by inserting crystal seeds into the trials (e.g. 13) however this requires the availability of crystals of the given protein or at least some crystalline material to start with. In an ongoing search for alternative heterogeneous

seeding materials, a variety of substances such as minerals (14), horse (15) and human (16) hair, thin films (17), charged surfaces (18, 19), mesoporous materials (20-22) and other materials (23) have been used as nucleants with varied success. The problem with such materials is that they are random substances, which have helpful properties such as porosity, nanostructure or electrostatic attractive potential, but no designed specificity for proteins. Our hypothesis was that MIPs would be very likely to serve as ideal nucleants, since they are designed to specifically attract their template protein.

This paper reports crystallization experiments performed with various model and target proteins, which demonstrate the effectiveness of MIPs as nucleants for protein crystallization. The mechanism of action of MIPs, based on atomic force microscopy measurements and on recent work on protein crystal nucleation is also discussed.

Results

Crystallization experiments

The MIPs made for this work are referred to as HydroMIPs (hydrogel based MIPs) since they are water-based and thus suitable for imprinting biological molecules (see Materials and Methods and SI). The HydroMIPs were imprinted with 7 proteins namely lysozyme, trypsin, catalase, haemoglobin, intracellular xylanase IXT6-R217W, alpha crustacyanin and human Macrophage Migration Inhibitory Factor (MIF). These will be referred to here as L-MIP, T-MIP, C-MIP, BHb-MIP, IX-MIP, AC-MIP and MIF-MIP, respectively. Nucleation inducing properties of the MIPs were investigated on 10 proteins. Each MIP was tested for its nucleation inducing capability on its own cognate protein as well as on others, as detailed in Tables 1, 2 and below. For every MIP created, a non-imprinted polymer (NIP) was also produced using the same procedure but without the protein template, in order to serve as a control for the MIP. Additional controls without any polymer were also set up.

Table 1 shows the results of experiments performed at metastable conditions. The crystallization conditions are detailed in *SI Materials and Methods*.

Complex of HIV proteins: Trials in the presence of L-MIP produced crystals that diffracted up to 4.2 Å. Previous attempts to crystallize this complex using conventional and non conventional methods, as well as known nucleating agents, had failed to produce crystals with diffraction beyond 9Å. T-MIP also produced crystals but not as well diffracting as the L-MIP.

Human MIF: crystals formed within 8 days at 1.15 M ammonium sulfate in the presence of MIF-MIP, L-MIP and T-MIP (Figure 1). All other trials remained clear for at least two months. At 1.10 M ammonium sulfate and below, all drops remained clear. At 1.20 M ammonium sulfate, drops with NIPs also gave crystals but the controls remained clear. At 1.25 M ammonium sulfate and above, all trials produced crystals, with crystals appearing faster in the drops containing MIPs. The crystals grown with MIF-MIP and T-MIP diffracted X-rays to a resolution of 1.2 Å using a rotating anode X-ray source. Previously, synchrotron sources were necessary to achieve the same resolution.

RECQ1: yielded crystals, the first appearing within two days, at 15% (w/v) PEG 3350, only in the presence of T-MIP. At 14% (w/v) PEG all trials remained clear for at least 3 weeks. At 16% (w/v) PEG 3350, drops with NIP also gave crystals after four days with the controls and drops containing L-MIP remaining clear. At 17% (w/v) PEG and above, all trials gave crystals. The ones with MIPs were obtained faster. The diffraction resolution limit of crystals grown in the presence of MIPS was 2.0Å compared with 2.3Å of crystals grown without MIPs.

Lysozyme: crystals formed within four days at 2.8% (w/v) sodium chloride only in the presence of L-MIP and T-MIP, but not in the presence of the other MIPs, NIP or in the controls. Below the metastable conditions at 2.7% (w/v) sodium chloride, all trials remained clear for at least six weeks after set up. At 2.9% (w/v), controls remained clear and drops with NIP also yielded crystals a day after the ones with MIP. At 3% (w/v) sodium chloride and above, which are labile conditions, all drops gave crystals, albeit sooner with the MIPs. The diffraction resolution limit of crystals grown in the presence and absence of MIPS was 1.5Å.

Trypsin: crystals formed within 7 days at 13% (w/v) PEG 8000, 0.2 M ammonium sulphate and 0.1 M sodium cacodylate at pH 6.5 only in the presence of T-MIP. Crystals also formed at 14% in the presence of T-MIP and L-MIP, but not in the presence of the other MIPs, NIP or in the controls. At 12% (w/v) PEG all drops remained clear and at 15% and above all trials gave crystals with crystals appearing

faster in the drops containing the MIPs. The diffraction resolution limit of crystals grown in the presence of MIPS was 1.5Å compared with 2.3Å of crystals grown without MIPs.

Thaumatin: crystals formed within 1 to 5 days at 0.3 M and 0.4 M sodium/potassium tartrate only in the presence of L-MIP and T-MIP. At 0.2 M Na/K tartrate, all trials remained clear for at least 4 weeks. All trials gave crystals at 0.5 M Na/K tartrate and above, albeit later in the controls. The diffraction resolution limit of crystals grown with MIPS was 1.5Å compared with 1.9Å of crystals grown without MIPs.

Haemoglobin: crystals formed within 5 days at 22.5% (w/v) PEG 3350 only in the presence of the BHb-MIP. At 20% (w/v) PEG 3350, all drops remained clear while at 25% (w/v) PEG 3350 all drops yielded crystals. In the controls and the drops containing NIPS they appeared after 7 days The diffraction resolution limit of crystals grown with MIPS was 2.8Å compared with 3.2Å of crystals grown without MIPs.

The X-ray diffraction patterns of crystals grown in drops containing the MIPs showed that these crystals diffracted to resolutions equivalent to, or better than their respective controls. This demonstrates that the MIPs do not interfere with diffraction quality.

Catalase did not show any nucleation-inducing effect from L-MIP, T-MIP, C-MIP or NIP. The nucleation of catalase was actually reduced by its own cognate MIP and to some extent by other MIPs as well.

Catalase is a special case. Its own cognate MIP inhibits nucleation although in some cases it sped up the nucleation of other proteins. Catalase crystallises via a different route, first precipitating with crystals forming later out of the precipitate. Catalase-imprinted polymer reduces the precipitation to levels that are not sufficient for crystal growth at lower supersaturations, possibly by excessively depleting the catalase solution. This has been corroborated by spectrophotometric measurements at 280 nm of the concentration of protein a few hours after setup at metastable conditions, in drops containing T-MIP, C-MIP and in controls. The concentration of protein was highest in controls (3.56 mg/ml), marginally lower in drops containing T-MIP (3.38 mg/ml) and appreciably lower in the presence of C-MIP (2.99 mg/ml). At higher supersaturations, C-MIP allows crystal growth when precipitation is already too heavy for crystallization without its presence. Other MIPs do not seem to promote

catalase nucleation. This may be due to the much higher size of the catalase molecule, making it a far worse binder to non-cognate MIPs, which thus neither promote nor inhibit its nucleation.

In order to compare the nucleation inducing capability of MIPs with other known nucleants, experiments were repeated at the same conditions in the presence of human hair, horse hair, zeolites and bioglass powder. No crystals were obtained in any of the trials containing these nucleants other than for lysozyme and trypsin which at these conditions produced small crystals in the presence of human hair, horse hair and the bioglass powder. The crystals obtained however, were multiple and small compared to large single crystals which appeared in the drops containing MIPs.

Figure 2 shows how the crystals often evolve from the MIP. Initially the drops with MIP are clear, after which there is a sequence of events: (i) first a separation of liquid phases occurs, forming protein-rich droplets on the MIP, which can reach a diameter of *ca.* 100 μm (Fig. 2a); (ii) after 6 days, crystalline aggregation is observed in these droplets (Fig. 2b); (iii) After 24 hours single, large and well-diffracting crystals appear from these protein-rich areas (Fig. 2b). The time of observing crystalline aggregation depends on the protein; for lysozyme and RECQ1 for example, the equivalent times were three days and one day respectively.

The application of MIPs for screening experiments

In order to test whether MIPs would also be effective in finding new hits during initial screening, 4 proteins were screened in the presence and in the absence of their cognate MIPs. These encompassed 3 target proteins (alpha crustacyanin, MIF and intracellular xylanase IXT6-R217W) and one model (trypsin). The Index screen was chosen for this investigation because it is a popular diverse reagent crystallization screen which is widely used. The above mentioned target proteins were selected since two of them have not produced useful crystals to date and the third (MIF) requires higher resolution crystals. The fourth, trypsin, which crystallises with relative ease, was included to act as a comparison.

Experiments using solutions 1-48 of the Index screen gave 4 to 5 hits for each of the 3 target proteins when their cognate MIPS were present (Table 2), whereas no hits were obtained in their absence. 4 hits were obtained in the case of alpha crustacyanin and 5 hits were attained for intracellular xylanase IXT6-R217W and MIF. In the case of trypsin the same 2 solutions produced hits with and without MIP. Only conditions which had crystals or crystallites were considered as hits (Figure 3a, 3b). The hits appeared between 24 hours and 4 days after setting up the trials. Control drops (i.e. without MIPs and drops containing NIPs) did not produce any hits after 4 weeks and beyond. Other known nucleants such as human hair (Fig. S1A), zeolites (Fig. S1B), horse hair and bioglass powder were tested at the conditions that gave hits with MIPs. Except in the case of trypsin these did not produce any hits after 4 weeks either.

The results demonstrate that in the presence of MIPs, 8-10% of the screening trials of the target proteins produced hits which would have been missed even when other nucleants were applied.

Additional trials were set up to see if non cognate MIPs would also give rise to the hits (Table 2). T-MIP and L-MIP were added to screening trials at the conditions that gave hits for the 3 target proteins and in the case of alpha crustacyanin, C-MIP was applied in addition to T-MIP and L-MIP due to the high molecular weight (320 kDa) of this protein. In the case of MIF, 2 hits were obtained with L-MIP and 3 hits with T-MIP. Intracellular xylanase IXT6-R217W produced 1 hit with T-MIP, and, as expected, no hits were obtained for alpha crustacyanin with these MIPs. The screening results are commensurate with those at metastable conditions in that MIPs of compatible size to the protein also give hits, albeit not as many as the cognate MIPs.

In order to test whether raising the concentration of the proteins would produce the hits without MIPs, all the trials which yielded hits were set up using 15- 30% higher concentrations of MIF and alpha crustacyanin. (The intracellular xylanase IXT6-R217W could not be concentrated above 8mg/ml, the concentration that was applied for the experiments). Screening with the higher concentrations of the two former proteins led to heavy precipitation meaning that the MIPs were not only revealing hits

which would have been otherwise missed, but also achieving this while consuming significantly lower concentrations of the proteins.

AFM Binding Measurements

The results above demonstrate that our hypothesis that MIPs would work as nucleants has materialized. To test this beyond the practical evidence of crystallization, atomic force measurements were performed to assess affinity of protein to the MIPs and compare it with affinity to NIP and also to a polylysine control surface.

In a study totally unrelated to protein crystallization, El Kirat et al. (24) have recently shown that atomic force spectroscopy could be used to probe polyacrylamide based MIPs used for cytochrome c imprinting of thin film MIPs attached to a mica surface. The atomic force measurements of the MIPs in our study were on the bulk gel MIPs that were used for the crystallization experiments (described in *SI Materials and Methods*). Non-imprinted polymer (NIP) and bovine haemoglobin (BHb) imprinted polymer were tested and a polylysine-coated coverslip acted as a control.

Figure 4 details representative force curves that were generated as a result of interactions that occurred between the AFM probes with BHb attached and the MIP sample. This is given as an exemplar figure of the hysteresis observed during the approach and retraction of the protein modified AFM tip onto the MIP surface. Force curves for NIP exhibited similar profiles and only differed in the force value. The distinctive, single peaked retraction curve displayed suggests that a single type of host-guest binding event is occurring.

One of the most powerful ways in which a MIP effect can be defined, is in relation to a NIP prepared in an identical manner to that of the MIP, but in the absence of the template molecule. For a given polymer surface, the repeat adhesion events were found to have a narrow force distribution about the mean force measured. We were able to discriminate between each polymer surface based on the force distributions recorded. A distinctive trend was observed. The polylysine control exhibited the smallest force, with a (mean) value of 13.51 nN (standard deviation ± 0.38) required to remove the AFM probe from the surface. A somewhat greater force of 18.90 nN (±

0.31) was required to withdraw the probe from the NIP surface. The increase in attractive forces exhibited between the two samples can be attributed to the BHb showing a greater affinity to the polyacrylamide than to the polylysine. Most significantly, a force of 23.08 nN (± 0.31) was required to withdraw the template-modified AFM tip from the cavity-containing MIP sample. This indicates that binding between these sites and the BHb molecule was occurring, which in turn resulted in a greater force being required to withdraw the tip from the sample. Literature values for single protein-pulling experiments typically show force values of 400-600 pN (25). Our values are significantly greater due to the cryogenic mode of preparation of the MIP and control samples. This was required in order to stabilise the hydrogel surfaces. The cryogenic preparation allows the surface to be frozen and the difference between the MIP and control surface remains the presence of cavities in the former and their absence in the latter. The results show that there is a stronger force of attraction between cognate protein-modified tip and MIP surface compared with control surfaces. The narrow standard deviation about the mean value measured for each surface adds further assurance that MIPs are behaving differently to control surfaces. It can therefore be concluded that highly specific interactions were reproducibly occurring with each sample investigated using this technique.

Discussion

It has been shown that crystal nucleation may proceed in two steps, namely aggregation of molecules into a dense fluid droplet and then ordering. This lowers the height of the energy barrier for nucleation: instead of a single, steep energy barrier which would occur if ordering of the molecules happened at the same time as their aggregation (the classical nucleation model), we would have two lower barriers if the two processes happened separately and in succession. We now have direct evidence of this mechanism, which ten Wolde & Frenkel (26) showed by simulation studies, Lutsko & Nicolis (27) by theoretical considerations and Vekilov (28, 29) by a variety of experimental and theoretical approaches. It seems that the MIPs, soon after their insertion (overnight for the cases of lysozyme, trypsin and RECQ1), promote aggregation of protein molecules, forming a protein-rich phase, which at a later stage becomes crystalline (Figure 2).

It therefore appears that in these cases, MIPs may function by facilitating the nucleation and stabilisation of droplets of the protein-rich liquid phase, at conditions which would be quite far from the liquid-liquid phase separation conditions in the absence of nucleant (i.e. in the bulk).

Lysozyme is one of very few proteins for which quantitative liquid-liquid demixing data has been obtained (30). From that data, it appears that liquid-liquid phase separation at 20 mg/ml lysozyme in sodium acetate buffer at pH 4.5 and 20°C (our conditions) requires at least 7 %(w/v) NaCl, instead of the 2.8 %(w/v) at which nucleation of protein-rich droplets and subsequently of crystals occurs in this study in the presence of MIP. The liquid-liquid demixing curve obtained at a concentration of 3 %(w/v) NaCl by Muschol & Rosenberger (30) gets very close to 0°C for 20 mg/ml lysozyme.

No quantitative liquid-liquid demixing data exists for the other proteins in this study. However, no visible droplets or clouding of the drops could be observed under the microscope at any time during the experiments in the absence of MIP, not only at metastable conditions but also well within the spontaneous nucleation zone of conditions. This qualitatively supports the general structure of a globular protein phase diagram proposed by Muschol & Rosenberger (30) and by Asherie (31), who place the liquid-liquid demixing curve in the bulk well beyond (at much higher supersaturations than) the solubility curve.

The MIP cavities, although they have a well-defined shape, are randomly dispersed through the gel. They therefore cannot induce the protein molecules to orient themselves in a specific pattern, i.e. providing a surface for epitaxial growth. It seems however, that the MIP can pull together a sufficient number of those molecules in order to overcome the energy barrier for the first step of forming a (yet disordered) precursor. The fabrication method is such that we expect a very high density of cavities due to the abundance of protein mixed with the monomer, making isolation of the cavities unlikely. The second step, ordering of the nucleus, may be aided by immobilised protein molecules in the cavities attracting further protein molecules. If the attractive forces between immobilised protein and protein in solution are similar in magnitude to the protein-polymer forces, then re-arrangement of the assembled

molecules to form ordered nuclei becomes possible in spite of the disorder in the cavities' orientations.

Another explanation of the effectiveness of the cavities that are not oriented in a way directly conducive to proper crystal packing, is the possibility of a statistical effect with only a few of the cavities in favourable mutual orientations. Various studies (32, 33) have shown that a very small number (less than 12) of macromolecules can be sufficient for the formation of a critical nucleus. This explanation is supported by the results, showing crystals forming on some parts of the MIP and not throughout it. This is actually an advantage, because we desire one or few crystals, rather than many. It may well be that there is a combination of the statistical effect with the lowering of the energy barrier.

An issue which may arise is that the imprints will be single isolated receptor sites, many of which will be partially or wholly buried in the polymer structure, thus not allowing the protein molecules to access them and also preventing the crystals from growing due to lack of space. Indeed, some of the pores will be buried due to the nature of the imprinting procedure. But, for the purpose of protein nucleation it does not matter that some are buried since only a few pores are needed at the surface for nucleation to occur. In order to ensure that some of the pores are on the surface, the imprinted hydrogels are broken into smaller particles thereby exposing cavities on the particle surface.

In summary, AFM results demonstrate that there is a definite binding of protein to the cavities of the MIPs and less so to the NIPs. The crystallization results follow this pattern, showing that in the presence of MIPs (i) crystals are formed in conditions that do not give crystals otherwise and (ii) crystals form faster in conditions which will produce crystals eventually. For crystals to grow in the presence of NIPs the crystallization conditions need to be at a higher supersaturation than in the presence of MIPs, thereby yielding poorer quality crystals.

We have demonstrated that MIP nucleants can be used in two ways: (i) as a heterogeneous seed for growing crystals in the metastable zone of the crystallization phase diagram, where crystals do not spontaneously nucleate but can often grow to

higher quality, and (ii) as an addition to standard screening conditions, where they can help to produce hits that would have been missed in their absence.

When embarking on the MIP experiments we expected that each MIP would work exclusively on its cognate protein and that it would be necessary to make a MIP for each protein to be crystallised. In practice, our results demonstrate that MIPs such as those imprinted with lysozyme and trypsin also induced the crystallization of other proteins with a molecular weight of the same order of magnitude. These observations promise further possibilities than initially envisaged, meaning that a MIP of one protein may be successfully used for other, size-compatible proteins. This is very important in the case of difficult to crystallise proteins, which are usually too scarce in supply for imprinting and would therefore benefit from the use of a related MIP.

The findings of this study open up a new scope for protein crystallization corroborating our hypothesis that by harnessing the proteins themselves as templates, MIPs are effective nucleation inducing substrates for both the screening and optimization stages of crystallization.

Materials and Methods

The materials required for the fabrication of the HydroMIP samples, the reagents utilised for the crystallization trials and the information pertaining to the preparation of the proteins tested are all documented within the Supporting Information (*SI Materials and Methods*).

HydroMIP fabrication

Traditional MIPs only demonstrate their selectivity when they rebind template in the organic solvent in which they were synthesised (34). These methods are therefore unsuitable for imprinting of biomolecules such as proteins, as they are denatured under such organic solvent conditions. The MIPs made for this work were therefore water-based MIPs, also referred to as hydrogel based MIPs (HydroMIPs). They offer a compromise between the polymerisation required for cavity formation and the need to keep protein structural integrity during imprinting. HydroMIPs are made of

polyacrylamide, a nitrogen containing member of the acrylate family of polymers, which is a suitable imprinting matrix for biological molecules, as it is water compatible, cheap, easily produced and can be derivatised to introduce functional groups (namely hydroxyl, carboxylate and amino groups) to better engineer the complementary interactions between the template molecule and the polymer (8).

HydroMIPs were prepared following a previously reported procedure (35) and with the intention of using as little protein sample as possible and at significantly smaller final volumes. For every MIP created, a NIP (non-imprinted polymer) was also created using the same material concentration as the MIP but without the protein template (*SI Materials and Methods*). The HydroMIPs and NIPs are translucent and have a gel-like appearance and texture.

Crystallization experiments

The MIPS and other nucleants (human hair, horse hair, zeolites VPI-5 and MCM-41, crushed glass and bioglass powder) were inserted into crystallization trials set up in hanging drops in either EasyXtal tools^{TM} (Qiagen) or Linbro plates. These drops consisted of 1 µl protein solution mixed with 1 µl reservoir solution. 0.2 µl of polymer (as a viscous gel) was then dispensed into these drops using a standard micropipette. The same polymer but not imprinted with protein (NIP) was also dispensed at the same conditions, as a control. An additional control without any polymer was also set up.

A simple "working phase diagram" was constructed for each protein (except for IXT6-R217W and alpha crustacyanin which were used only for the screening experiments) in order to find metastable conditions. Protein concentrations and buffers were kept fixed and supersaturation was varied by spanning a range of precipitating agent concentrations. It was ensured that a suitable range of conditions, spanning from undersaturation to spontaneous nucleation was being searched in each case.

For each protein and each tested condition, trials were set up at the same time from the same batch of protein at identical crystallization conditions with MIP imprinted

with lysozyme (L-MIP), trypsin (T-MIP), catalase (C-MIP), haemoglobin (BHb-MIP), MIF (MIF-MIP), as well as with NIP and without polymer. Each combination was repeated in at least 6 different drops. Detailed methodology and the precise range of conditions for each of the proteins are documented in the Supporting Information (*SI Materials and Methods*).

Solutions 1-48 of the Index screen (Cat. No. HR2-144, Hampton Research, USA) were used for screening experiments of trypsin, alpha crustacyanin, MIF and intracellular xylanase IXT6-R217W (details of the stock protein solutions are given in *SI Materials and Methods*). The experiments were incubated at room temperature (ca. 22°C) and all trials that gave hits were repeated in at least duplicate to ensure reproducibility.

The HIV Complex, RECQ1, thaumatin and trypsin crystals were X-rayed at the Diamond Light Source on the MX beamline I04. MIF, lysozyme and haemoglobin crystals were X-rayed on the Rigaku 007HF-M X-ray generator at Imperial College London, operating at 40 kV and 30 mA, with VHF optics producing a spot size of less than 100 microns, Saturn 944+ CCD detector and Oxford Cryosystems 700 liquid nitrogen cryostream.

Acknowledgements

This work was supported by the UK Engineering and Physical Sciences Research Council (EPSRC) grant EP/G014736/1 and EP/G014299/1 and the European Commission OptiCryst project LSHG-CT-2006–037793. M. Swann is thanked for introducing SMR and NEC. We thank D.A. Veselkov, J. Bergeron, M. Malim, I. Laponogov and M.R. Sanderson for the HIV complex, O. Gileadi for RECQ1, V. Solomon, O. Tabachnikov and Y. Shoham for intracellular xylanase IXT6-R217W and P. Zagalsky for alpha crustacyanin.

References

(1) Arshady R, Mosbach K. (1981) Synthesis of substrate selective polymers by host-guest polymerization. *Makromolekulare Chemie*182:687-92

(2) Sellergren B (2000) Imprinted polymers with memory for small molecules, proteins or crystals. *Angew. Chem. Int. Ed.* 39:1031-1037.

(3) Sellergren B, Ekberg B, Mosbach K (1985) Molecular imprinting of amino acid derivatives in macroporous polymers : demonstration of substrate- and enantio-selectivity by chromatographic resolution of racemic mixtures of amino acid derivatives. *Journal of Chromatography A* 347:1-10.

(4) Nilsson KG I, Sakaguchi K, Gemeiner P, Mosbach K (1995) Molecular imprinting of acetylated carbohydrate derivatives into methacrylic polymers. *Journal of Chromatography A* 707:199-203.

(5) Suedee R et al (1998) Thin-layer chromatography using synthetic polymers imprinted with quinine as chiral stationary phase. *Journal of Pharmaceutical and Biomedical Analysis* 11:272-276.

(6) Shi HQ, Tsai WB, Garrison MD, Ferrari S, Ratner BD (1999) Molecular imprinted polymers for biorecognition of bioagents. *Nature* 398:593-597.

(7) Hillberg AL, Tabrizian M (2008) Biomolecule imprinting: developments in mimicking dynamic natural recognition systems. *ITBM-RBM* 29:89-104

(8) Liao J-L, Wang Y, Hjerten S (1996) A novel support with artificially created recognition for the selective removal of proteins and for affinity chromatography. *Chromatographia* 42:259-262.

(9) Hansen DE (2007) Recent developments in the molecular imprinting of proteins. *Biomaterials* 28:4178-4191.

(10) Bruggemann O (2002) Molecularly imprinted materials - receptors more durable than nature can provide. *Adv Biochem Eng* 76:127-163.

(11) Chayen NE, Saridakis E (2008) Protein crystallization: from purified protein to diffraction-quality crystal. *Nat Methods* 5:147-153.

(12) Chayen NE (2004) Turning protein crystallization from an art into a science. *Curr Opin Struct Biol* 14:577-583.

(13) Bergfors T (2003) Seeds to crystals. *J Struct Biol* 142:66-76.

(14) McPherson A, Shlichta P (1988) Heterogeneous and epitaxial nucleation of protein crystals on mineral surfaces**.** *Science* 239:385-387.

(15) D'Arcy A, Mac Sweeney A, Haber A (2003) Using natural seeding material to generate nucleation in protein crystallization experiments**.** *Acta Cryst D* 59:1343-1346.

(16) Georgieva DG, Kuil ME, Oosterkamp TH, Zandbergen HW, Abrahams JP (2007) Heterogeneous nucleation of three-dimensional protein nanocrystals. *Acta Cryst D* 63:564- 570.

(17) Pechkova E, Nicolini C (2002) Protein nucleation and crystallization by homologous protein thin film template**.** *J Cell Biochem* 85:243-251.

(18) Nanev CN (2007) On the slow kinetics of protein crystallization. *Cryst Res Technol* 42:4-12.

(19) Falini G, Fermani S, Conforti G, Ripamonti A (2002) Protein crystallization on chemically modified mica surfaces. *Acta Cryst D* 58:1649-1652.

(20) Chayen NE, Saridakis E, El-Bahar R, Nemirovsky, Y (2001) Porous silicon: an effective nucleation-inducing material for protein crystallization. *J Mol Biol* 312:591-595.

(21) Henschel A, Huber P, Knorr K (2008) Crystallization of medium-length 1-alcohols in mesoporous silicon: an x-ray diffraction study. *Phys Rev E* 77:042602.

(22) Chayen NE, Saridakis E, Sear RP (2006) Experiment and theory for heterogeneous nucleation of protein crystals in a porous medium. *Proc Natl Acad Sci USA* 103:597-601.

(23) Saridakis E, Chayen NE (2009) Towards a 'universal' nucleant for protein crystallization. *Trends Biotechnol* 27:99-106.

(24) El Kirat K, Bartkowski M, Haupt K (2009) Probing the recognition specificity of a protein molecularly imprinted polymer using force spectroscopy. *Biosens Bioelectron* 24:2618-2624.

(25) Lv Z, Wang J and Chen G (2010) Probing specific interaction forces between human IgG and rat anti-human IgG by self-assembled monolayer and atomic force microscopy. *Nanoscale Res Lett* 5:1032-1038

(26) ten Wolde PR, Frenkel D (1997) Enhancement of protein crystal nucleation by critical density fluctuations. *Science* 277:1975-1978.

(27) Lutsko JF, Nicolis G (2006) Theoretical evidence for a dense fluid precursor to crystallization. *Phys Rev Lett* 96:046102.

(28) Vekilov PG (2004) Dense liquid precursor for the nucleation of ordered solid phases from solution. *Cryst Growth Des* 4:671-685.

(29) Vekilov PG (2005) Two-step mechanism for the nucleation of crystals from solution. *J Cryst Growth* 275:65-76.

(30) Muschol M, Rosenberger F (1997) Liquid-liquid phase separation in supersaturated lysozyme solutions and associated precipitate formation/crystallization. *J Chem Phys* 107:1953-1962.

(31) Asherie N (2004) Protein crystallization and phase diagrams. *Methods* 34:266-272.

(32) Galkin O, Vekilov PG (2000) Are nucleation kinetics of protein crystals similar to those of liquid droplets? *J Am Chem Soc* 122:156-163.

(33) Tsekova D, Popova S, Nanev C (2002) Nucleation rate determination by a concentration pulse technique: application on ferritin crystals to show the effect of surface treatment of a substrate. *Acta Cryst D* 58:1588-1592.

(34) Stevenson D (1999) Molecular imprinted polymers for solid-phase extraction. *Trends Analyt Chem* 18:154-158.

(35) Hawkins DM, Stevenson D, Reddy SM (2005) Quantification and confocal imaging of protein specific molecularly imprinted polymers. *Anal Chim Acta* 542:61-65.

Figure Legends

Figure 1. MIF crystallization trials in the presence of trypsin-imprinted polymer (T-MIP) and the non-imprinted polymer (NIP). The MIP and NIP have a translucent gel-like appearance. When added to crystallization drops they spread out and can fragment. (a) A single MIF crystal grown in a drop containing T-MIP. The MIP is indicated by the arrow. Scale bar corresponds to 0.1mm (b) Drop containing NIP at identical conditions; no crystals are formed. Scale bar corresponds to 0.15 mm.

Figure 2. Progression of the formation of trypsin crystals on trypsin-imprinted MIP. (a) phase separation (b) crystalline aggregation at the protein-rich droplets (bottom left) and large single crystal. Scale bars correspond to 0.05mm.

Figure 3. Results of screening with the Index screen.
(a) a hit containing MIF crystals in solution 5, scale bar corresponds to 0.15mm (b) a hit containing alpha crustacyanin crystals in solution 43, scale bar corresponds to 0.05mm The color of the alpha crustacyanin protein is blue, hence the dark color of the crystals.

Figure 4. A typical force-distance graph detailing the interrogation of MIP with a BHb-conjugated 10nm (radius of curvature) silicon nitride AFM probe. The grey line shows the tip descending, initially without contact with the surface. At some point, the tip jumps into contact with the surface and indents into it. The black line shows the tip retracting: the adhesion/bonding between tip and sample causes the cantilever to adhere to the sample. As the retraction continues the adhesion breaks. The cycle can then be repeated.

Table Legends

Table 1. Crystallization results at metastable conditions. Controls consist of the same conditions without MIPs or NIPs.

Table 2. Hits obtained in screening trials using MIPs. ✓ represent hits. The hit conditions are listed in *SI Materials and Methods*.

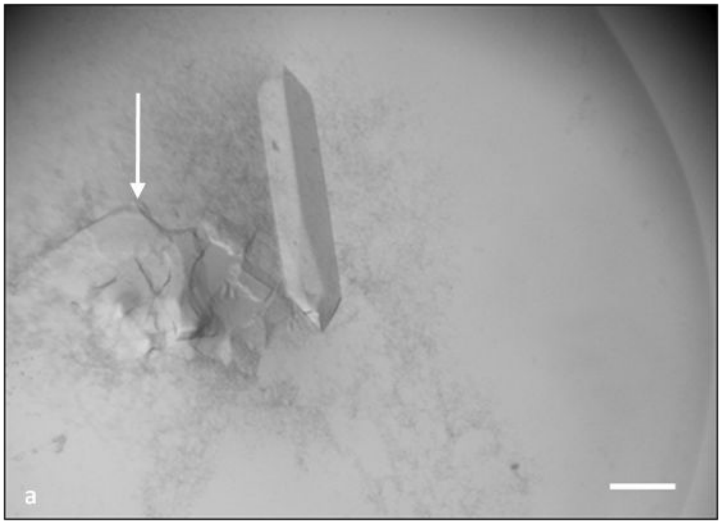
a

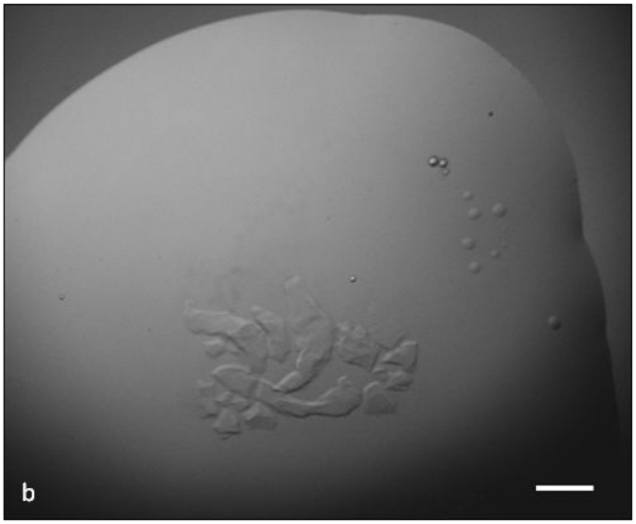
b

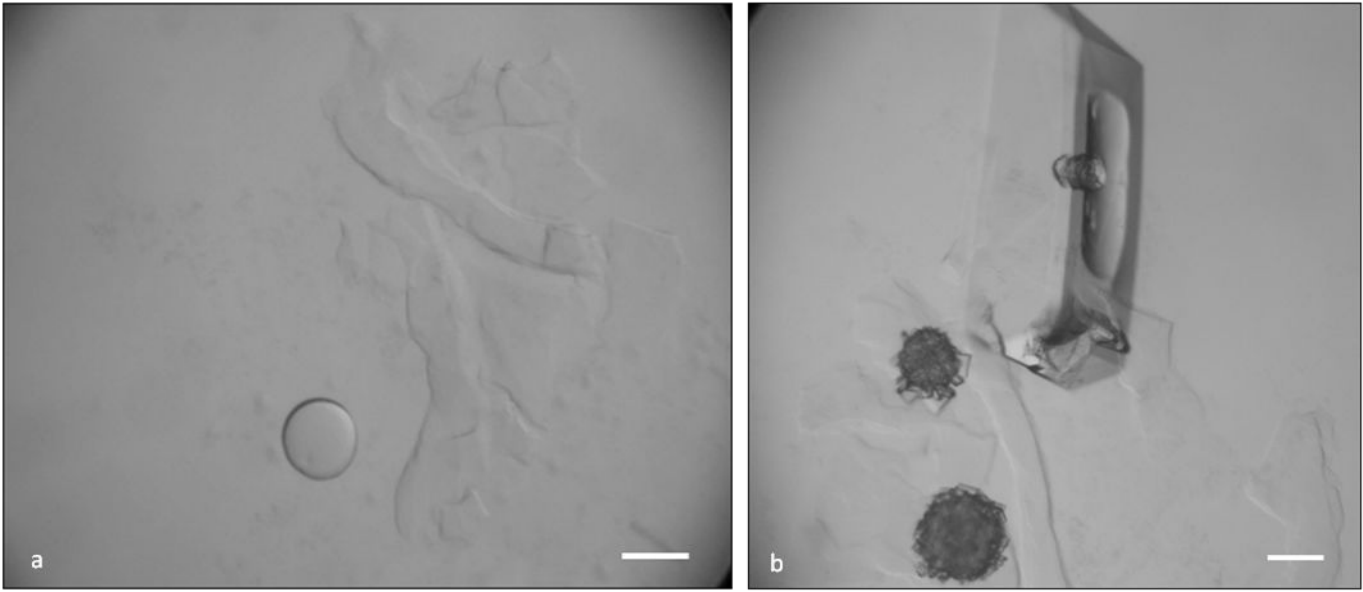
a
b

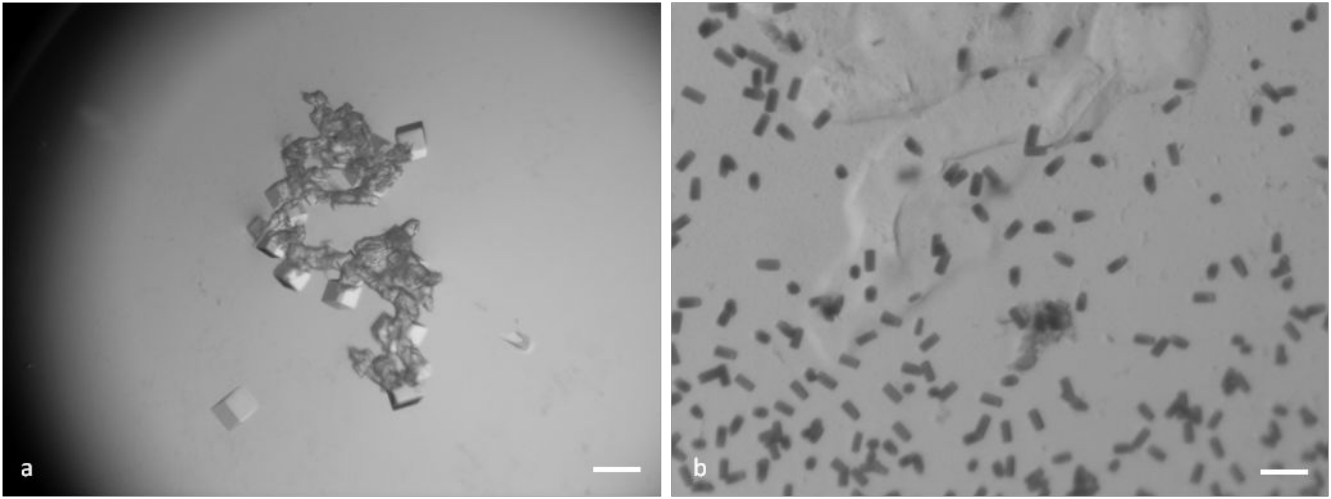
a
b

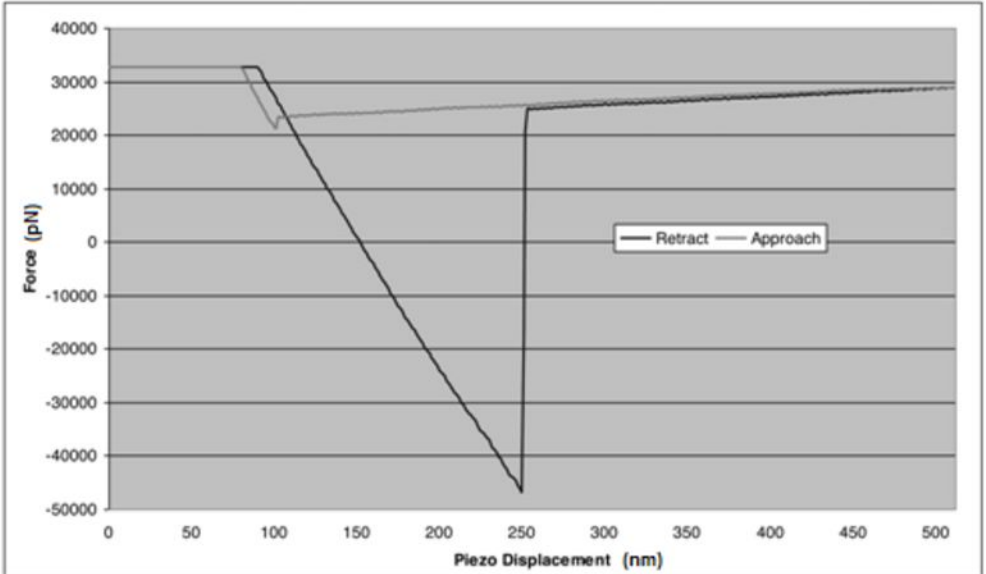
40000
30000
20000
10000
0
-10000
-20000
-30000
-40000
-50000
Force (pN)
0
50
100
150
200
250
300
350
400
450
500
Piezo Displacement (nm)
Retract
Approach

Table 1.

Protein	M.W. (kDa)	L-MIP	T-MIP	C-MIP	MIF-MIP	BHb-MIP	NIPS	Controls
Human MIF	12.3	crystals	crystals	-	crystals	-	clear	clear
Lysozyme	14.5	crystals	crystals	clear	clear	clear	clear	clear
Thaumatin	22	crystals	crystals	clear	clear	clear	clear	clear
Trypsin	24	clear	crystals	clear	clear	clear	clear	clear
HIV Complex	35.2	crystals	crystals	clear	-	clear	clear	clear
Haemoglobin	64.5	clear	clear	-	clear	crystals	clear	clear
RECQ1	67.2	clear	crystals	-	-	-	clear	clear
Catalase	232	clear	clear	clear	-	-	clear	clear

Table 2

Protein	Conc mg/ml	Index screen solution	Cognate MIP	L-MIP	T-MIP
MIF 12.3 kDa	12	4	✓	✓	✓
		5	✓	✓	✓
		6	✓	-	-
		8	✓	-	-
		27	✓	-	✓
IXT6 R217W 38.6 kDa	8	19	✓	-	-
		23	✓	-	✓
		26	✓	-	-
		30	✓	-	-
		31	✓	-	-
Crusta--cyanin 320 kDA	10	41	✓	-	-
		43	✓	-	-
		44	✓	-	-
		46	✓	-	-